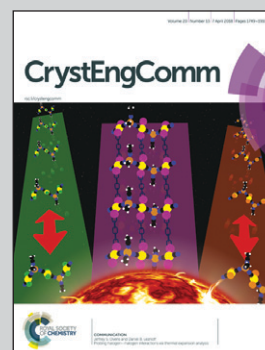


Showcasing research work by Dániel Vajk Horváth, Tamás Holczbauer\*, Laura Bereczki, Roberta Palkó, Nóra Veronika May, Tibor Soós and Petra Bombicz from the Research Centre for Natural Sciences, Hungarian Academy of Sciences, Budapest, Hungary.

Polymorphism of a porous hydrogen bond assisted ionic organic framework

iHOF structures are presented, where anion $\cdots\pi$  interactions support the hydrogen bonds forming non-covalently bonded organic frameworks of high porosity occasionally with organic linkers. The role of the molecular inflexibility in framework construction is proved.

As featured in:



See Tamás Holczbauer *et al.*, *CrystEngComm*, 2018, 20, 1779.



[rsc.li/crystengcomm](http://rsc.li/crystengcomm)

Registered charity number: 207890

Cite this: *CrystEngComm*, 2018, 20, 1779Received 9th January 2018,  
Accepted 26th February 2018

DOI: 10.1039/c8ce00041g

rsc.li/crystengcomm

The polymorphism of a porous, non-covalently bonded ionic organic framework is reported. The framework is constructed by hydrogen bonding and anion $\cdots\pi$  interactions. In a solvatomorphic lattice, pyridine takes part in the framework formation. The role of molecular rigidity in framework construction is proven by analogous non-porous crystals, where polymorphism also appears.

Solid structures with large volume areas have a broad range of applications such as sensing,<sup>1</sup> drug delivery,<sup>2</sup> heterogeneous catalysis,<sup>3,4</sup> separation,<sup>5</sup> storage,<sup>6</sup> etc.<sup>7</sup> We describe the polymorphism and solvatomorphism of porous cationic molecular crystals constructed by the assistance of C–H $\cdots$ Br<sup>−</sup> and Br<sup>−</sup> $\cdots\pi$  interactions. The rigid molecular conformation achieved by C–H $\cdots\pi$  intramolecular interactions is a condition of the constructed framework, which is proven by comparing structures of related more flexible molecules crystallising into different non-porous architectures. Polymorphism occurs in the case of both porous and non-porous packing arrangements (Scheme 1, Table 1).

The design of highly ordered porous architectures has attracted wide interest owing to their broad application. They are chemically diverse materials whose macroscopic properties can be tailored. The discovery of metal organic frameworks (MOFs)<sup>7–10</sup> opened a new branch of research. Most recently, liquid phase MOFs<sup>11</sup> were reported. Covalent organic frameworks (COFs)<sup>12,13</sup> are crystalline porous polymers. Porous hydrogen-bonded organic frameworks (HOFs) have come to the forefront of interest in recent years.<sup>14–16</sup> The basic building blocks of HOFs mainly consist of two parts: a scaffold and hydrogen bonding interaction sites.<sup>17</sup>

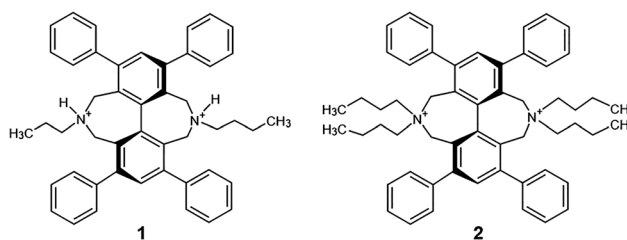
## Polymorphism of a porous hydrogen bond-assisted ionic organic framework†

Dániel Vajk Horváth, <sup>ID</sup><sup>a</sup> Tamás Holczbauer, <sup>ID</sup><sup>\*ab</sup> Laura Bereczki, <sup>ID</sup><sup>b</sup> Roberta Palkó, <sup>ID</sup><sup>a</sup> Nóra Veronika May, <sup>ID</sup><sup>b</sup> Tibor Soós <sup>ID</sup><sup>a</sup> and Petra Bombicz <sup>ID</sup><sup>b</sup>

A well-orchestrated interplay of intermolecular forces, molecular inflexibility and the presence of symmetry characterize the non-covalently bonded organic frameworks.

Most of the organic frameworks described are electronically neutral. The design principles and applications of ionic metal–organic frameworks (iMOFs)<sup>18</sup> and ionic covalent organic frameworks (iCOFs)<sup>19</sup> were recently published. The ions inside the channels of the skeletons can be utilized for specific interactions with guest molecules, like increased efficiency and selectivity in ion exchange. During the development of ionicity of iMOFs, the role of the metal ion or cluster and the choice of the ligand are decisive. iCOFs with ionic linkers and neutral knots are reported.<sup>19</sup> Two types of ionic frameworks can be distinguished by the nature of the backbone: anionic and cationic.

The long-range periodicity in crystals of HOFs is a product of the directionally specific short-range intermolecular interactions. Understanding molecular recognition principles is important to control the self-assembly of HOFs.<sup>20</sup> It is beneficial to prevent  $\pi\cdots\pi$  stacking, which is against void formation.<sup>14</sup> A diversity of hydrogen bonds and supramolecular interactions of carboxylic, hydroxyl, amine and amide groups



**Scheme 1** The peripheral substituents of compound **1** (butyl and phenyl groups) are flexible and disordered. The dimorphs of the neutral form, as well as the HCl salt of **1**, are all closely packed crystal structures. The molecular conformation of **2** is anchored by intramolecular C–H $\cdots\pi$  interactions (butyl:phenyl, 1:1); thus, its HBr salt is able to form cationic organic frameworks assisted by hydrogen bonds.

<sup>a</sup> Institute of Organic Chemistry, Research Centre for Natural Sciences, Hungarian Academy of Sciences, Magyar tudósok körútja 2, 1117 Budapest, Hungary.

E-mail: holczbauer.tamas@ttk.mta.hu

<sup>b</sup> Chemical Crystallography Research Laboratory, Research Centre for Natural Sciences, Hungarian Academy of Sciences, Magyar tudósok körútja 2, 1117 Budapest, Hungary

† Electronic supplementary information (ESI) available. CCDC 1813220–1813225. For ESI and crystallographic data in CIF or other electronic format see DOI: 10.1039/c8ce00041g





**Table 1** Some crystal data and void characteristics of **1a**, **1b**, **1c**, **2a**, **2b** and **2c** (more information in Table S1)

	<b>1a</b>	<b>1b</b>	<b>1c</b>	<b>2a<sup>d</sup></b>	<b>2b<sup>d</sup></b>	<b>2c<sup>d</sup></b>
Space group	$P\bar{1}$	$P2_1/n$	$P2_1/c$	$Fddd$	$Pnna$	$P2_1/n$
<i>a</i> [Å]	12.2542(11)	15.0148(17)	12.4240(8)	22.071(3)	24.343(3)	17.465(3)
<i>b</i> [Å]	12.3204(11)	9.6841(11)	23.0450(15)	25.991(3)	15.987(4)	15.707(3)
<i>c</i> [Å]	12.4610(11)	25.874(3)	15.1970(8)	28.554(4)	17.571(5)	25.981(4)
$\alpha$ [°]	91.981(7)	90	90	90	90	90
$\beta$ [°]	106.699(7)	100.421(3)	99.050(7)	90	90	110.398(3)
$\gamma$ [°]	93.107(7)	90	90	90	90	90
<i>V</i> unit cell [Å <sup>3</sup> ]	1796.9(3)	3700.1(7)	4296.9(4)	16 380(4)	6838(3)	6680(2)
<i>V</i> void [Å <sup>3</sup> ]	0	80	335	6864 <sup>a</sup>	2666 <sup>a</sup>	2398/1221 <sup>a,b</sup>
[%]		2%	8%	42% <sup>a</sup>	39% <sup>a</sup>	36%/18% <sup>a,b</sup>
Pore <sup>c</sup> [cm <sup>3</sup> g <sup>-1</sup> ]	0	0.018	0.069	0.556 <sup>a</sup>	0.433 <sup>a</sup>	0.358/0.181 <sup>a,b</sup>
KPI [%]	68.6	66.4	61.6	41.2 <sup>a</sup>	46.2 <sup>a</sup>	56.7/47.5 <sup>a,b</sup>
<i>Z'</i> for 1 or 2	1	1	1	1/4	1/2	1
Final <i>R</i> indices	$R_1 = 0.0471$ , $wR^2 = 0.1044$	$R_1 = 0.0681$ , $wR^2 = 0.1306$	$R_1 = 0.0787$ , $wR^2 = 0.1945$	$R_1 = 0.2302$ , $wR^2 = 0.5471$	$R_1 = 0.1047$ , $wR^2 = 0.2801$	$R_1 = 0.1276$ , $wR^2 = 0.3386$
<i>R</i> indices (all data)	$R_1 = 0.0777$ , $wR^2 = 0.1257$	$R_1 = 0.1207$ , $wR^2 = 0.1512$	$R_1 = 0.1205$ , $wR^2 = 0.2219$	$R_1 = 0.2968$ , $wR^2 = 0.5847$	$R_1 = 0.1862$ , $wR^2 = 0.3288$	$R_1 = 0.2138$ , $wR^2 = 0.3937$

<sup>a</sup> Without THF. <sup>b</sup> Without pyridine/with pyridine. <sup>c</sup>  $V_{\text{void}}/(\rho_{\text{calc}} \times V_{\text{unitcell}})$ . <sup>d</sup> Because of the high void volumes, Platon SQUEEZE software was used during the refinement.

often serve as hydrogen-bonded motifs of HOFs.<sup>5</sup> A useful method to increase the strength of the hydrogen bond is to incorporate charged sites to assist hydrogen bonding of the building blocks. The interaction between an electron deficient arene and an anion has been recognised recently as a non-covalent interaction.<sup>21,22</sup>

Polymorphism is only occasionally observed in the family of porous frameworks. Free energy differences between polymorphic forms are usually small.<sup>23</sup> Polymorphs differ in their relative thermodynamic stabilities which are influenced by temperature and pressure. The polymorphic transformation changes the adsorption properties of a framework, and polymorphism is associated with the so-called “breathing effect”.<sup>24</sup> Polymorphs differ in their crystal packing arrangements and/or in the conformation of the molecules – there are different supramolecular interactions and crystallographic symmetries in the lattices of different polymorphic forms.<sup>23</sup>

An iCOF formed from 4,4',4'',4'''-(pyrene-1,3,6,8-tetrayl)-tetraaniline (PyTTA) as a neutral knot with an organic cationic bromide linker was reported very recently.<sup>19</sup> Stable anion... $\pi$  interaction complexes of naphthalene diimides (NDI) with chloride and bromide in the gas phase were reported not long ago.<sup>25</sup> These two achievements suggested that hydrogen bond-assisted ionic organic frameworks can be prepared by the application of a modified Maruoka type organocatalyst containing a diazadibenzo[*ef,k,l*]heptalene skeleton. Maruoka achieved outstanding efficiency and enantioselectivity in alkylation reactions with chiral phase-transfer catalysts owing to a BINOL backbone (Fig. S38 and Table S8, ESI†).<sup>26,27</sup> The main molecular structural characteristics of ammonium salt catalysts are their large aromatic moieties, structural rigidity and marked axial chirality. The quaternary ammonium cation part of the catalyst has now been duplicated, and the aromatic moiety moved from the edge of the

molecule to the centre. In the two newly synthesized Maruoka-type phase-transfer catalysts reported here, the two reaction centres of the symmetrical molecules were formed by the ring closure of rigid, seven-membered rings in the last step of the synthesis. One or two butyl groups (**1** and **2**) are attached to the saturated ring nitrogen (Scheme 1). The molecules are fully substituted with apolar phenyl and alkyl groups. The synthesized model compounds were used in framework construction experiments and can also be a promising new family of Maruoka-type catalysts with further modifications. The 3D open pore framework structure is advantageous in catalytic activity.

Both compounds **1** and **2** were synthesised (Scheme S1, ESI†) starting from the inexpensive chalcone **3** and dimethyl-1,3-acetonedicarboxylate **4**. Michael addition and subsequent condensation of the dinucleophile **4** with the dielectrophile **3** gave the cyclohexanone derivative **5**. This compound was transformed into the tetrasubstituted iodobenzene **7** via the tosylhydrazone intermediate **6** in a Bamford–Stevens type one pot reaction, followed by *in situ* oxidation with 50% yield. The polysubstituted iodo compound **7** gave the biphenyl **8** via the Ullmann homocoupling reaction. The ester functional group was reduced to **9** and brominated to give the tetrabromo compound **10**. This intermediate was subjected to ring closure with butylamine or dibutylamine to give compound **1** or **2**.

The 5,11-dibutyl-1,3,7,9-tetraphenyl-4,5,6,10,11,12-hexahydro-5,11-diazadibenzo[*ef,k,l*]heptalene (**1**) molecule is substituted by only one butyl substituent at each N atom. By single crystal X-ray structure determination, the neutral dibutyl derivative shows dimorphism (**1a**:  $P\bar{1}$ , **1b**:  $P2_1/n$ ). In the partially flexible molecules, one of the butyl groups is disordered in both structures. It is attributed to the remaining flexibility of the semi-rigid molecule, due to the lack of anchoring intramolecular interactions of the substituents,



because of the uneven butyl to phenyl (2:4) ratio. The external surface of **1** is highly apolar. C–H $\cdots\pi$  interactions stabilize the lattices. In its HCl salt, 5,11-dibutyl-1,3,7,9-tetraphenyl-4,5,6,10,11,12-hexahydro-5,11-diazadibenzo[*ef,k*l]-heptalene-5,11-diium-chloride (**1c**;  $P2_1/n$ ), the residual space among the flexible substituents attached to a stiff scaffold allows parts of the molecule: one butyl and two terminal phenyl groups, to be disordered. N–H $\cdots\text{Cl}^-$  and C–H $\cdots\text{Cl}^-$  interactions are present in the lattice. Neither the dimorphs of the neutral molecule (**1a**, **1b**) nor its HCl salt (**1c**) are able to build a framework structure. The flexibility of the molecule (**1**) does not support the formation of an organic framework structure.

In spite of the general expectations, the introduction of the second butyl group on the ring nitrogen reduces the flexibility of the 5,5,11,11-tetrabutyl-1,3,7,9-tetraphenyl-4,5,6,10,11,12-hexahydro-5,11-diazadibenzo[*ef,k*l]heptalene-5,11-diium bromide (**2**) molecule with increasing steric crowding. The molecule is strained by four C–H $\cdots\pi$  intra-molecular interactions between each butyl and the neighbouring terminal phenyl substituents (butyl:phenyl, 4:4) (Fig. 1).

The crystal lattices of **2** are highly ordered porous solid-state architectures formed by supramolecular self-assembly *via* non-covalent interactions.

Simple recrystallization of the HBr salt from tetrahydrofuran results in two polymorphic frameworks (**2a**;  $Fddd$ , Fig. 2, and **2b**;  $Pnna$ , Fig. 3). Void volumes are **2a**: 42% and **2b**: 39%, respectively, in the highly porous systems. The rigid, conformationally highly similar molecules pack differently in the dimorphic architectures.

The organic frameworks are assisted by the interactions formed between C $_{\text{ain}}$ –H and Br $^-$  as charge-assisted hydrogen bonds, as well as by anionic Br $^-$  $\cdots\pi$  interactions with the electron deficient central phenyl ring (Fig. 1).

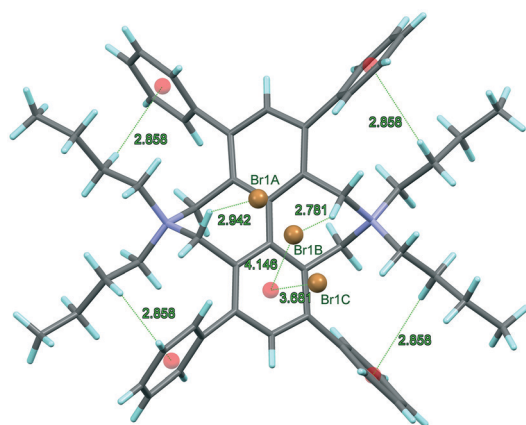


Fig. 1 The C $_{\beta\text{ex}}$ –H $\cdots\pi$  intramolecular interactions responsible for the rigidity of the molecule in the framework structure of **2a**. The C $_{\alpha\text{in}}$ –H $\cdots\text{Br}^-$  and Br $^-$  $\cdots\pi$  interactions contribute to the framework architecture. Br $^-$  is disordered in **2a**. In **2b** and **2c**, the molecular symmetry decreases losing one (**2b**) and two (**2c**) twofold symmetries, but the same kinds of intra- and intermolecular interactions are present, while Br $^-$  is not disordered.

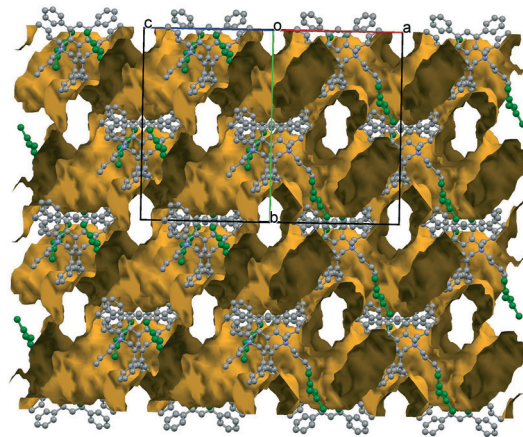


Fig. 2 The 3D sponge-like crystal structure of **2a** ( $Fddd$ , 42%), one of the iHOF dimorphs. The bromide anions are coloured green. The channels are filled with disordered THF.

By applying additional solvent pyridine to THF, a novel highly porous structure appears, whose void volume is 36%. In this solvatomorphic form (**2c**;  $P2_1/n$ ; Fig. 4 and 5), pyridine molecules become part of the cationic framework with C–H $_{\text{ph-ex}}$  $\cdots\pi$  secondary interactions as neutral linkers between the cationic knots. It is in contrast to published iCOFs with ionic linkers and neutral knots.

Conformational symmetry appears, showing two (**2a**) or one (**2b**) twofold symmetry axis in the molecule. The lattice symmetry and the molecular symmetry of the rigid scaffold decrease correspondingly, having 1/4 (**2a**,  $Fddd$ ), 1/2; (**2b**,  $Pnna$ ) and 1 (**2c**,  $P2_1/n$ ) structural unit in the asymmetric unit of the polymorphs and the solvatomorphic form.

In conclusion, the presented crystal structures illustrate the polymorphism of a porous, hydrogen bond-assisted ionic organic framework, iHOF (**2a** and **2b**). The framework is constructed by C–H $\cdots$ halogenide ions and the recently described anion $\cdots\pi$  interactions. A solvatomorph of the

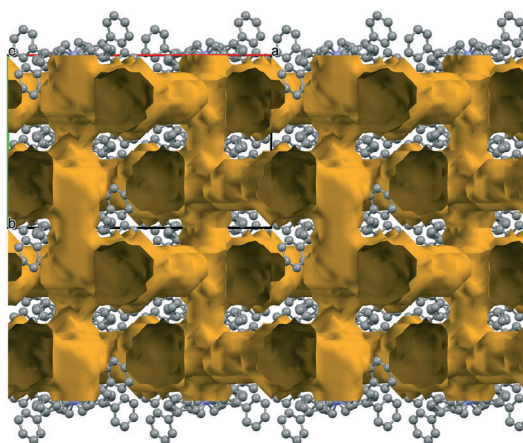


Fig. 3 The framework structure of **2b** ( $Pnna$ , 39%), the other member of the iHOF dimorphs. The bromide anions are coloured green. The channels are filled with disordered THF.



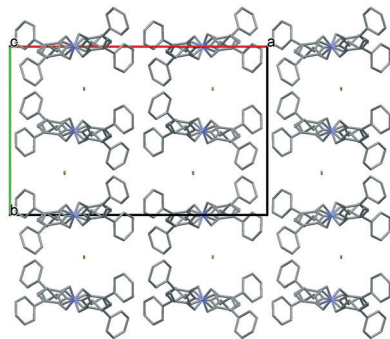


Fig. 4 Packing arrangement of the cationic framework **2b** ( $Pnna$ ). It is greatly similar to **2c**. **2b** crystallizes in a higher symmetry space group than **2c** ( $Pnna$  is a supergroup of  $P2_1/n$ ). The additional twofold symmetry also becomes a molecular symmetry in **2b**.

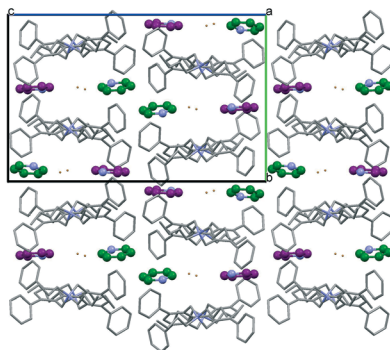


Fig. 5 Packing arrangement of the framework **2c** ( $P2_1/n$ ) with cationic knots. Pyridine molecules (purple and green) take part in the framework construction as neutral linkers. The incorporation of the pyridine as the building block reduces the symmetry of the lattice and the scaffold.

framework is prepared (**2c**), where the pyridine molecules take part in the formation of the framework. The role of the molecular rigidity in framework construction is demonstrated by the non-porous crystal structures of related more flexible molecules (**1a–1c**), where polymorphism also appears (**1a** and **1b**).

This work was supported by the National Research, Development and Innovation Office-NKFIH through OTKA K115762, K116150 and K124544, as well as by the J. Bolyai Research Scholarship of the Hungarian Academy of Sciences (TH).

## Conflicts of interest

There are no conflicts to declare.

## Notes and references

- 1 T. Kusukawa and M. Fujita, *J. Am. Chem. Soc.*, 2002, **124**, 13576–13582.

- 2 M. Vallet-Regí, F. Balas and D. Arcos, *Angew. Chem., Int. Ed.*, 2007, **46**, 7548–7558.
- 3 J. S. Seo, D. Whang, H. Lee, S. I. Jun, J. Oh, Y. J. Jeon and K. Kim, *Nature*, 2000, **404**, 982–986.
- 4 J. Lee, A. Hu and W. Lin, *J. Am. Chem. Soc.*, 2002, **124**, 12948–12949.
- 5 D. N. Dybtsev, H. Chun, S. H. Yoon, D. Kim and K. Kim, *J. Am. Chem. Soc.*, 2004, **126**, 32–33.
- 6 R. E. Morris and P. S. Wheatley, *Angew. Chem., Int. Ed.*, 2008, **47**, 4966–4981.
- 7 M. J. Prakash and M. S. Lah, *Chem. Commun.*, 2009, 3326–3341.
- 8 O. M. Yaghi and G. Li, *Angew. Chem., Int. Ed. Engl.*, 1995, **34**, 207–209.
- 9 L. Zhu, X.-Q. Liu, H.-L. Jiang and L.-B. Sun, *Chem. Rev.*, 2017, **117**, 8129–8176.
- 10 G. Mehlana, G. Ramon and S. A. Bourne, *Microporous Mesoporous Mater.*, 2016, **231**, 21–30.
- 11 R. Gaillac, P. Pullumbi, K. A. Beyer, K. W. Chapman, D. A. Keen, T. D. Bennett and F.-X. Coudert, *Nat. Mater.*, 2017, **16**, 1149–1154.
- 12 M. Dogru and T. Bein, *Chem. Commun.*, 2014, **50**, 5531–5546.
- 13 C. S. Diercks and O. M. Yaghi, *Science*, 2017, **355**, 923–930.
- 14 Y.-F. Han, Y.-X. Yuan and H.-B. Wang, *Molecules*, 2017, **22**, 266–300.
- 15 H. Wang, Z. Bao, H. Wu, R.-B. Lin, W. Zhou, T.-L. Hu, B. Li, J. C.-G. Zhao and B. Chen, *Chem. Commun.*, 2017, **53**, 11150–11153.
- 16 W. Yan, X. Yu, T. Yan, D. Wu, E. Ning, Y. Qi, Y.-F. Han and Q. Li, *Chem. Commun.*, 2017, **53**, 3677–3680.
- 17 F. M. A. Noa, S. A. Bourne, H. Su and L. R. Nassimbeni, *Cryst. Growth Des.*, 2017, **17**, 4647–4654.
- 18 A. Karmakar, A. V. Desai and S. K. Ghosh, *Coord. Chem. Rev.*, 2016, **307**, 313–341.
- 19 N. Huang, P. Wang, M. A. Addicoat, T. Heine and D. Jiang, *Angew. Chem., Int. Ed.*, 2017, **56**, 4982–4986.
- 20 G. Resnati, E. Boldyreva, P. Bombicz and M. Kawano, *IUCrJ*, 2015, **2**, 675–690.
- 21 X. Lucas, A. Bauzá, A. Frontera and D. Quinonero, *Chem. Sci.*, 2016, **7**, 1038–1050.
- 22 M. Giese, M. Albrecht and K. Rissanen, *Chem. Commun.*, 2016, **52**, 1778–1795.
- 23 P. Bombicz, *Crystallogr. Rev.*, 2017, **23**, 118–151.
- 24 D. Aulakh, J. R. Varghese and M. Wriedt, *Inorg. Chem.*, 2015, **54**, 8679–8684.
- 25 R. E. Dawson, A. Hennig, D. P. Weimann, D. Emery, V. Ravikumar, J. Montenegro, T. Takeuchi, S. Gabutti, M. Mayor, J. Mareda, C. A. Schalley and S. Matile, *Nat. Chem.*, 2010, **2**, 533–538.
- 26 M. Kitamura, S. Shirakawa and K. Maruoka, *Angew. Chem., Int. Ed.*, 2005, **44**, 1549–1551.
- 27 S. Shirakawa, K. Liu and K. Maruoka, *J. Am. Chem. Soc.*, 2012, **134**, 916–919.

